http://journal.rmutp.ac.th/

Flexural Performance of Corroded Reinforced Concrete Beams Repaired with CFRP Sheets

Arnon Wongkaew*

Faculty of Engineering, Burapha University
169 Longhard Bangsaen, T. Saensuk, A. Maung, Chon-Buri 20131

Received 27 September 2020; Revised 30 March 2021; Accepted 5 May 2021

Abstract

Corrosion of steel reinforcements in concrete is one of the main causes of early deterioration and reduction of service loads of reinforced concrete (RC) structures. This paper reports the results of an experimental program that was carried out to evaluate the effect of reinforcement corrosion on the flexural performance of RC beams, and to investigate the efficiency of externally bonded carbon fiber reinforced polymer (CFRP) sheets to repair the corrosion-damaged RC beams. Seven RC beams with the same cross section and reinforcement details were prepared, including the control beam (B0). First, tension reinforcements of six RC beams were corroded by using an accelerated impress-current process to obtain corrosion levels of 15%, 30%, and 50% of weight loss, according to Faraday's law. Then, three beams were repaired using CFRP sheets attached to the bottom surface, leaving the other three unrepaired. All beams were subjected to the four-point bending load test. The experimental results show that the corrosion specimens demonstrated a significant deterioration on the structural performance and the integrity by decreasing in their ultimate load capacity, stiffness, and ductility. The deterioration by corrosion of tension reinforcements can be successfully overcome using CFRP sheets as the repair material. The technique can restore the beam strength to its original design strength, except specimen B50F2 having severe steel-corrosion damage of 50%. A conservative value of the ultimate bending capacity of the beams with low corrosions (15%-30%) can be predicted by using RC conventional models, as suggested in ACI 318. However, the opposite trend is obtained for the high corrosion beam (50%). Appling ACI 440.2R provision to predict the ultimate flexural capacity of corroded beams repaired with CFRP sheets shows rather fair values for low corrosions (15%-30%), but significantly overestimates the strength of the high corrosion beam (50%).

Keywords: Externally Bonded Carbon Fiber Reinforced Polymer (CFRP) Sheets; Corrosion; Reinforced Concrete Beam; Repair; Flexural Strength

**** Corresponding Author. Tel.: +668 4892 3773, E-mail Address: arnonw@eng.buu.ac.th***

1. Introduction

One of the main problems of reinforced concrete (RC) structures is the deterioration of concrete material due to corrosion of steel reinforcements induced by chloride, especially under severe marine environments. This corrosion problem has been well recognized by many researchers affecting the mechanical behavior of RC structures, such as stiffness, serviceability, ductility, and load-carrying capacity. It can lead to further structural distress due to the loss of the reinforcing steel cross-sectional area as well as their bond strength [1]. As a result, the RC structures damaged by corrosion may have inadequate strength up to their service loads, otherwise to unexpected loading such as strong wind, wave, even small ground movement. Nowadays, there are many innovative materials and techniques introduced for the RC structural rehabilitation. Externally bonded fiber reinforced polymer (FRP) sheets is one of the most efficient new materials among those rehabilitation materials for RC structures. Initially, the FRP sheet was introduced to the solution for strengthening RC columns, mainly. It has been examined in many literatures to improve strength, ductility, and even energy absorption capacity of the RC columns. Later on, since its effectiveness, there also are many applications to strengthen other RC members such as beam, slab, joint, etc.

Many studies were concentrated on the effects of corrosion and its degree on the flexural, shear strength, and mechanical behavior of RC beams. Researchers [1-7] showed their results from the experiments that the corroded RC beams with either the laboratory-accelerated corrosion process or under a chloride environment demonstrated significant loss of their yield, ultimate, shear, and ductility capacity depending on the level of corrosion in their reinforcement steels. One of the main reasons of those reductions caused from the deterioration of the bond strength between steel and concrete [1]. The deflection of control RC beams subjected to 30 days of accelerated corrosion increased by 40%-70% with 6% of the mass loss of their reinforcements [2]. The ultimate moment capacity of corroded beams was reduced linearly by approximately 0.7% with respect to every 1% of the corrosion increment [3]. The load carrying capacity and the stiffness of the beams decreased with the increase of the corrosion level [4, 6]. Long term corrosion process done under 26-years chloride environment showed a shift failure mode from shear to flexural failure due to the large effect of corrosion [5].

On the other side, there have been some studies on the rehabilitation technique of using the externally bonded CFRP sheets to restore the load carrying capacity of the corroded RC beams. Al-Saidy et al. [7] used CFRP sheets to repair the corroded beams. Results showed the repaired RC beams was capable of reaching their original designed load capacities. U-wrap CFRP sheets were utilized to retrofit RC beams with corrosion damage [8]. The flexural load and stiffness capacity of the corroded beams were successfully increased.

To elaborate the use of externally bonded FRP sheets as a rehabilitation

technique for corrosion-damaged RC beams available to engineers and owners in order to confidently select this method for such a work, this study is aimed with the objectives of 1) to investigate the electrochemical process on corrosion of tensile reinforcing steel of RC beams with 3 three different levels of weight loss 15%, 30%, and 50% of steel reinforcements, 2) to experimentally determine the structural behavior and ultimate strength of defected and repaired RC beams, 3) to evaluate the use of externally bonded CFRP sheets as a repair methodology of the corrosion-damaged RC beams.

2. Experimental Program

2.1 Accelerated Corrosion Process

An electrochemical process was used to accelerate the corrosion of steel reinforcements of RC beams [1]-[9]. First, the RC beams with 28-day concrete strength were partially submerged in a cement tank with 5% concentrate of sodium chloride solution. A power supply with a direct current (DC) of a maximum output of 35 amperes (A) at 12 volts (V) was used for this process. The tensile reinforcements were connected to the positive side (Anode) and the stainless steel rod was connected to the negative side (Cathode) of the DC power supply. The desired degrees of corrosion were set to 15%, 30%, and 50% of their original weights. A common method to determine targeted levels of corrosion employed in this study is based on Faraday's Law. The theoretical mass of rust produced per unit of surface area could be determined using Faraday's law [2] as illustrated in equation (1)

$$\Delta W = \frac{I.t.A_m}{Z.F} \quad (1)$$

where

ΔW = weight loss of steel bar (g)
I = electrical current applied (Ampere)
t = time for desired weight loss (Second)
A_m = atomic weight of steel 55.85 g/mol
Z = the valence of the reaction equal 2
F = Faraday's constant (96,500 Coulomb/mol)

A schematic diagram and experimental setup of the accelerated corrosion process is shown in **Fig.1**. In order to successfully obtain the different levels of reinforcement corrosion of 15%, 30%, and 50%, the relationship between duration of the impressed current (t) and the applied current (I) was regularly monitored within 6 hours a day. It is important to note that the current can't be kept constant, therefore, weight loss of steel need to be recalculated daily. **Fig.1** also demonstrates an example of applied current (I) plotted against time (t). The areas under the curve were calculated using a graphical analysis software. The acceleration process was terminated when the targeted corrosion levels reached.

During a corrosion process of steel, a swelling of steel bars can be expected because of increasing of their volumes. This can lead to significant expansive forces generated in concrete as shown in **Fig.2**. Then, further spalling and cracking

of concrete cover can be projected and speeding acceleration of reinforcement deterioration, even more.

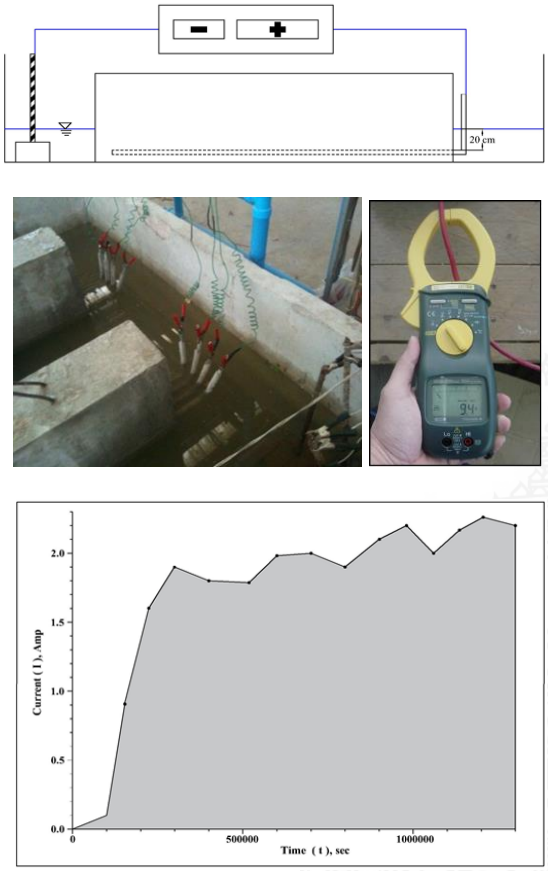

Fig. 1 Acceleration corrosion process

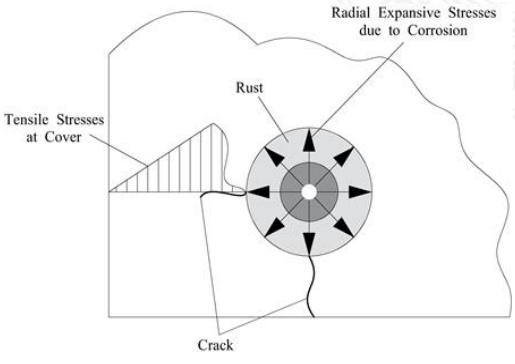

Fig. 2 Tensile stresses and crack at concrete cover due to corrosion

2.2 Repair Technique

The externally bonded carbon fiber reinforced polymer (CFRP) composite sheet was utilized as a rehabilitation technique for this study. The repair processes were classified depending on the levels of corrosion as a low level of 15% and 30%, and a high level of 50%. For the low corrosion level, there was nothing additionally applied to the beams, except cleaning the remaining undamaged concrete surface by using a grinder and air blower. Then, the CFRP sheets were directly attached to those bottom beam surfaces. On the other hand, for the high corrosion level beam, the deteriorated concrete was removed and replaced using the high strength cement, SikaMicro SCC. As well as, the corroded reinforcing steels were replaced with new steel bars of the same diameter. **Fig. 3** illustrates CFRP sheets were applied to the bottom surfaces of beams as shown in **Fig. 4**. Electrical strain gauges were also attached to the top and bottom surface of concrete, as well as the outer surface of CFRP sheets at the middle span length of beam as shown in **Fig. 4**. It should be noted that all repair processes were done by specialists from SIKA product.

Fig. 3 Repair of specimens group 2

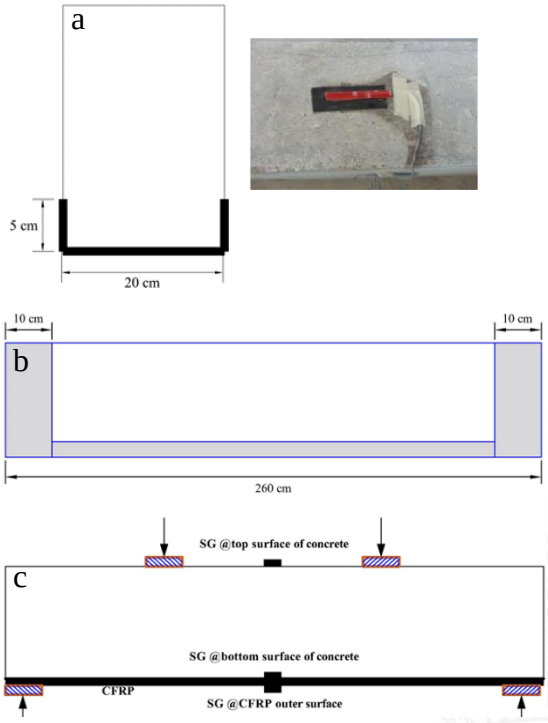

Fig. 4 CFRP sheet and strain gauge locations

2.3 Test Setup

A flexural test was performed for all beam specimens supported over a span of 2400 mm under the displacement control of the four-point transverse load scheme up to failure. The test was performed using an Universal Testing Machine with the maximum load capacity of 1500 kN. The beams were simply supported on top of a custom-made steel H-beam. The four-point loading scheme was applied by a hydraulic actuator through a load cell of 500 kN placed at the center of the other custom-made loading steel H-beam. The vertical displacement of the beams was monitored using LVDT attached at the bottom of the middle span of the beams, directly in line with the load cell. All test data from the load cell, LVDT, and actuator were stored automatically in a data logger connected to those instruments. All specimens were painted with a white color to observe crack development and marking. **Fig. 5** illustrates the test setup sketch along with a photo picture in the laboratory.

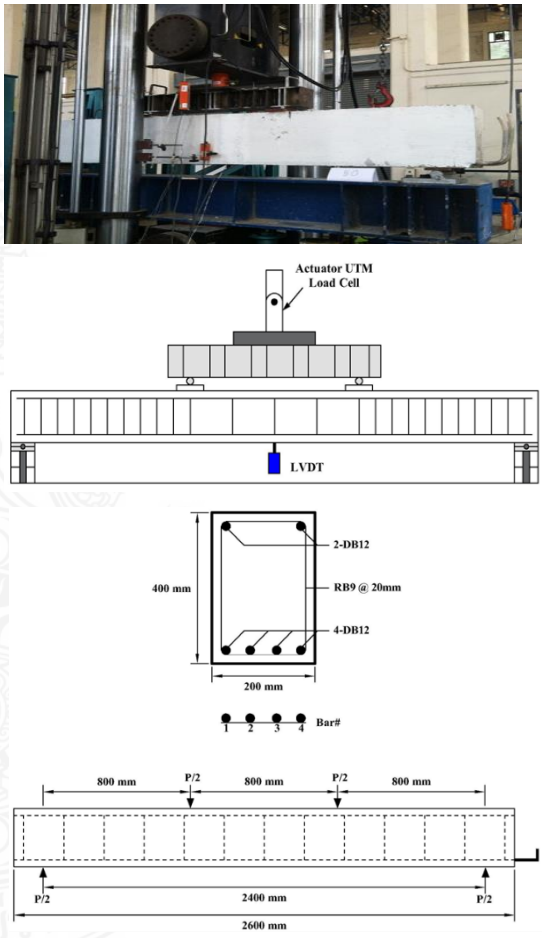

Fig. 5 Experimental and instrumentation setup

2.4 Material Properties

A ready mixed concrete with normal cylinder strength of 24 MPa was used to cast all RC beam specimens. Deformed

steel bars used as a main reinforcement have a nominal yield stress of 400 MPa and ultimate tensile stress of 600 MPa. Rounded steel bars with a nominal yield stress of 240 MPa and ultimate tensile stress of 400 MPa was used as stirrup bars. All repair materials SIKA products was selected as the repair materials for this study. SikaWrap300C, SikaDur330, and SikaMicro SCC were used as CFRP sheets, epoxy, and cement grout, respectively. The mechanical properties of materials used in this study such as concrete, steel, CFRP sheets (SikaWrap300C), SikaMicro SCC, and Sikadur330 can be seen from **Table 1**. The mechanical properties of all Sika products are also available online.

Table 1 Mechanical properties of materials used in this study

Material	Yield Strength (MPa)	Ultimate Strength (MPa)	Elastic Modulus (MPa)
Steel (DB)	400	600	200,000
Steel (RB)	240	400	200,000
Concrete	-	24	-
SikaWrap 300C	-	3500	220,000
SikaDur 330	-	30	3800[1]
SikaMicro SCC	-	26[2] 380[3]	-

([1] in flexural, [2] 3 days, [3] 7 days)

2.5 Specimen Details

The experimental work was conducted at the structural laboratory of civil engineering department, Burapha University. Seven RC beams with a cross-section of 200×400 mm with a supported span length of 2400 mm were tested under the four-point transverse load up to failure. Dimensions and reinforcement details of beam specimens are shown in **Fig. 5**. Four 12 mm diameters deformed bars and two other bars with same diameters were used as longitudinal tension and compression reinforcements, respectively. For stirrups, 9 mm diameters rounded bar was placed at a spacing of 20 mm along the span length. The experiments were categorized into two groups as presented in **Table 2**. Group1 consists of the control (Undamaged) specimen and the corrosion-damaged specimens with weight loss of tension steels by 15%, 30%, and 50% of their original weights, named as B0, B15, B30, B50. Group2 represents the same set of repaired specimens by using a technique of the externally bonded CFRP composite sheets, given as B15F1, B30F1, B50F2.

Table 2 Repair details of specimens

Group	Beam	Desired Weight Loss (%)	CFRP Layer
1*	B0	0	No
	B15	15	No
	B30	30	No
	B50	50	No
2**	B15F1	15	1
	B30F1	30	1
2***	B50F2	50	2

* No repair of concrete and steel

** and *** label the low and high corrosion levels, respectively. Their repaired methodologies are described in topic 2.2.

3. Experimental Results and Discussion

3.1 Actual Weight Loss of Steel Bar

The electrical current (I) applied to each steel bar as shown in **Fig. 1** and time

Table 3 Area under *I-t* curves of steels

Beam	Area Under Curves *I-t* (Amp. x Sec.) *10^6				
	Bar# 1	Bar# 2	Bar# 3	Bar# 4	Sum #1-4
B0	NA	NA	NA	NA	NA
B15-1	2.30	1.14	0.34	2.24	6.03
B15-2	0.91	1.72	0.99	2.30	5.93
B30-1	2.60	3.30	3.40	2.73	12.1
B30-2	0.42	2.40	4.26	3.06	15.4
B50-1	3.97	6.40	3.37	5.74	19.5
B50-2	12.8	3.97	2.32	7.01	26.1

Table 4 Desired and actual weight loss of steel for beam specimens

Beam	Initial Weight W_i (g)	Loss Weight ΔW (g)	Desired Weight Loss (%)	Actual Weight Loss (%)
B0	9413	0	0	0
B15-1	9413	1743.21	15	18.52
B15-2	9413	1715.14	15	18.22
B30-1	9413	3480.35	30	36.97
B30-2	9413	4443.11	30	47.20
B50-1	9413	5635.64	50	59.87
B50-2	9413	7553.35	50	80.24

(*t*) for desired weight loss are presented in **Table 3**. To calculate the actual weight loss of steel bar, the corroded reinforcement bas were removed from all tested specimens after the flexural tests, and labeled. Then, the steel bars were cleaned and re-weighted without any dust. Since the initial weights of each steel bars were recorded before casting. Therefore, the actual weight loss of steels from the corrosion process can be computed according to equation (1). As can be seen from **Table 4**, the actual weight losses are higher than the desired corrosion values predicted from equation (1) with average discrepancy under 10%, except B50-2 with 30.24%. Since the applied current was not switched off on the schedule; therefore, it leaded to more weight loss than original anticipation.

3.2 Load-Deflection Responses

A comparison of load-displacement responses at the middle span of specimens for each group is given in **Fig. 6a**. The load-displacement was obtained from LVDT and the load cell attached to test specimens as presented in **Fig. 5**. As seen, three response regions can be clearly identified, corresponding to the moment-curvature diagram of a typical reinforced beam subjected to a bending moment [13]. The control beam (B0) prematurely failed with a maximum load of 209 kN at a displacement of 9.1 mm. This failure load was rather different from an ultimate load calculated by the designed equation from ACI 318 [11] without a strength reduction factor (ϕ) as shown in **Table 5** (152 kN). The specimens B15 and B30 have almost identical responses including crack, yield, and ultimate loads, except values of B15 slightly higher shown in **Fig. 6b**. Also, the stiffness in the service stage of B15 was somewhat similar to B30. Therefore, it leads to conclude that no significant loss of the flexural capacity of beams B15 and B30 was detected from this experiment. Nevertheless, the beam B50, the specimen with the highest corrosion, displayed a significant reduction in all loading stages. It failed prematurely due to a rupture of the corroded tensile steel reinforcements.

As shown in **Fig. 6c**, after repairing of B15 and B30 by externally applied CFRP sheets to the surface of the bottom concrete, significant increment of the

yield and ultimate loads were observed. Besides, the deflections at the yield and ultimate loads of these two specimens also occurred at the same value. The stiffness and the load responses at the yield and ultimate points of B15F1 were much higher than those of B30F1, clearly causing from the lower corrosion levels in the steel reinforcements of B15F1. For B50F2, major enhancement of the yield and ultimate loads were noticed from the test result, but in contrast of deflection. Although F50F2 with two layers of CFRP sheets initially showed higher stiffness than B30F1, its stiffness started to decay until reaching the ultimate load, resulting from debonding of the epoxy material.

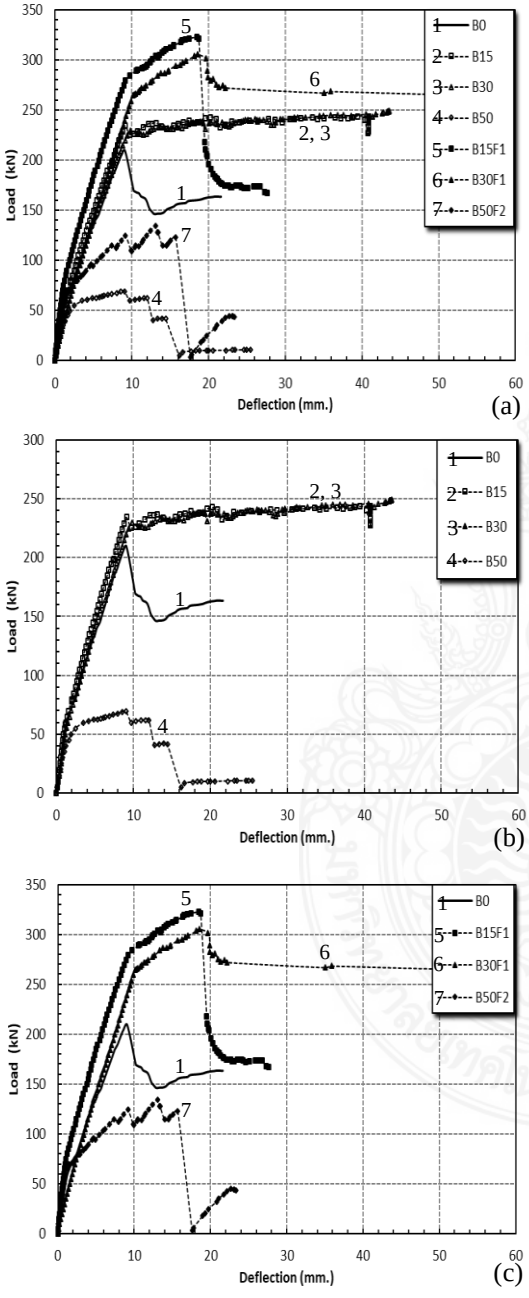

Fig. 6 Comparison of load-displacement responses (a) overall, (b) group1, (c) group2

The experimental and theoretical comparison of the ultimate load, along with the relative load capacity ratios between the test and computed results based on the flexural capacity of beam cross sections are listed in **Table 5**. The ultimate loads of beams, B0, B15, B30, and B50 are computed by ACI 318 [11]. The corresponding values for beams B15F1, B30F1, and B50F2 are calculated from ACI 440.2R [12]. These ultimate values are computed without the strength reduction factor (ϕ). All theoretical ultimate loads were calculated using material properties available from **Table 1** with the assumption of bond-perfect RC beams by neglecting the actual bond characteristic, the corrosion damage in the longitudinal reinforcements and the contacted stirrups, and damage in the surrounding concrete. The effect of weight loss of longitudinal reinforcements is incorporated to calculation by reducing in the steel diameters, equivalently to 85%, 70%, 50% of their original sizes, with respect to B15-B15F1, B30-B30F1, B50-B50F2. The mechanical properties of

Sika products are available online. Some necessary parameters of SikaWrap 300C for computing the flexural moment capacity are available in Table 1. Also, its thickness of 0.167 mm per one layer and the laminate elongation at break in tension of 1.59% are obtained from the product data sheet.

Table 5 Ultimate load comparison between experiment and ACI code

Beam	Ultimate Load (ACI) P_n kN	Ultimate Load (Exp.) P_u kN	Relative Load Capacity Ratio P_n/P_u
B0	152	NA*	NA*
B15	129	238	0.54
B30	107	245	0.44
B50	78	70	1.11
B15F1	302	323	0.93
B30F1	285	305	0.93
B50F2	271	134	2.02

Exp. = Experiment

NA* = Test data is either unavailable.

As seen from **Table 5**, theoretical ultimate loads of B15 and B30 are in the range of 44%-54% of measured from the experiments. It shows that ACI 318 design provision predicts quite conservative values of the ultimate load capacity (P_n) for the low corrosion beams. Oppositely observed with the high corrosion beam, B50, the ultimate load computed by ACI gives about 11.1% higher than the result from the experiment. ACI 440.2R design provision slightly underestimates the ultimate loads by margin of 7% for both B15F1 and B30F1, and significantly overestimates the ultimate capacity of B50F2 by 102%.

Comparison of load increment between non-repaired corroded beams and those repaired with CFRP sheets are shown in **Table 6**. It can be concluded that the reduction of the yield and ultimate load is clearly detected with the increasing corrosion. Moreover, the externally bonded CFRP sheets efficiently enhance the stiffness and strength of corroded beams.

Table 6 Load increments

Beam	Load Increments (%)	
	Yield	Ultimate
B15	235	238
B15F1	279	323
%	18.72	35.71
B30	230	245
B30F1	260	305
%	13.04	24.49
B50	55	70
B50F2	60	134
%	9.10	91.94

The crack, yield, and ultimate loads from the experiment are summarized in **Table 7**. Since the control beam (non-corroded beam), B0, tested data was unavailable, the comparison made within the different levels of corrosion are discussed instead. For the low corroded beams, B15 and B30, the results on yield, and ultimate loads are almost the same, with less than 3% discrepancy, and 10% difference for the crack load. However, significant reduction of those loads can be detected with the high corroded beam, B50, comparing to average values of B15 and B30, by approximation of 50%, 74%, and 72% for the crack, yield, and ultimate loads, correspondingly. The ratio of

ultimate to yield capacity of the corroded beams shows increment of the load capacity ranging from 1%, 7%, and 27% with respect to 15%, 30%, and 50% corrosion. This post-yielding performance of corroded beams was caused from the tensile behavior of the corroded steel bars suggested by the pervious literature [5].

Table 7 Loads from the experiment

Beam	Crack Load (kN)	Yield Load P_y (kN)	Ultimate Load P_u (kN)	P_u/P_y
B0	60	NA*	NA*	NA*
B15	50	235	238	1.01
B30	55	230	245	1.07
B50	20	55	70	1.27
B15F1	NA*	279	323	1.16
B30F1	NA*	260	305	1.17
B50F2	NA*	60	134	2.23

NA* = Test data is either unavailable.

For the corroded beams with CFRP sheets, B15F1 and B30F1 exhibited almost the same yield and ultimate load capacity with less than 8% and 6% difference. During the post-yielding behavior, B15F1 and B30F1 showed 16% and 17% increasing in the load capacity. Moreover, the strong post-yielding behavior was observed from B50F2 with 123% load increment. However, after the ultimate loads, sharp drop of the load capacity was noticed for all three CFRP beams, corresponding to the delamination failure of the fiber material. For B50F2, two load jumps were observed during the post-yielding period resulting from redistribution of the load capacity from concrete to CFRP sheets at the support.

3.3 Ductility

The impact of corrosion on the mechanical behavior of the beams was reported using the ductility index. The ratios of displacements at the yield and ultimate load extracted from **Fig. 6** were calculated and shown in **Table 8**. Since the control beam (B0) prematurely failed, a comparison with B0 was unavailable from this study. The results clearly indicate that ductility decreases from 4.39 to 3.64 when the corrosion levels increased from 15% to 50%. Especially, B50 has ductility decreasing by 17%, and 11% with respect to B15 and B30. The beams with CFRP sheets, B15F1 and B30F1 display ductility of 2.01. Much higher ductility of 8.73 can be founded from B50F2. Nevertheless, no clear conclusion can be made on the effect of CFRP sheets to improve ductility of the corroded beams. It seems that CFRP sheets has no effect to ductility improvement for the low corrosion beams, B15 and B30. On the other hand, significant ductility enhancement of 140% can be detected for the high corrosion beam, B50.

Table 8 Deflection, and ductility of the experiment specimens

Beam	Deflection at Yield (Δ_y) mm	Deflection at Ultimate (Δ_u) mm	Ductility (Δ_u/Δ_y)
B0	NA*	NA*	NA*
B15	9.1	40	4.39
B30	9.8	40	4.08
B50	2.5	9.1	3.64
B15F1	9.2	18.5	2.01
B30F1	9.9	18.5	2.01
B50F2	1.5	13.1	8.73

NA* = Test data is either unavailable

3.4 Failure Mode

A typical failure pattern of a beam subjected to a fourth-point load test was illustrated in **Fig. 7**, described as follows. Type 1 fails by flexural failure of the bottom tensile reinforcement in which a ratio of the tensile reinforcement is low. Type 2 fails by crushing of top concrete where a ratio of the tensile reinforcement is high. Type 3 is shear failure which significantly induces from insufficient or high spacing of the stirrup reinforcement. Type 4 fails by a combination of flexural failure of the bottom tensile reinforcement and shear failure.

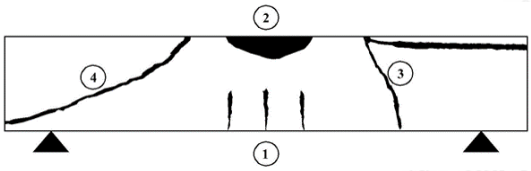

Fig. 7 Typical failure pattern of a beam subjected to a fourth-point load test [9]

Fig. 8 is the photos of tested specimens, B0, B15, B30, B50, B15F1, B30F1, B50F2, relatively. For group1, when the load was gradually applied to the beams, multiple flexural cracks appeared perpendicular to the bottom surface in the middle third span of the tension zone, and started to propagate and widen. Flexural yielding followed by concrete crushing occurred for all specimens in this group, except B0 and B50. The flexural-shear crack of B0 was so severe leading to failure before crushing of compression surface of the beam. On the other hand, B50 failed by significantly widen of the vertical crack perpendicular to the bottom surface and following with a rupture of the

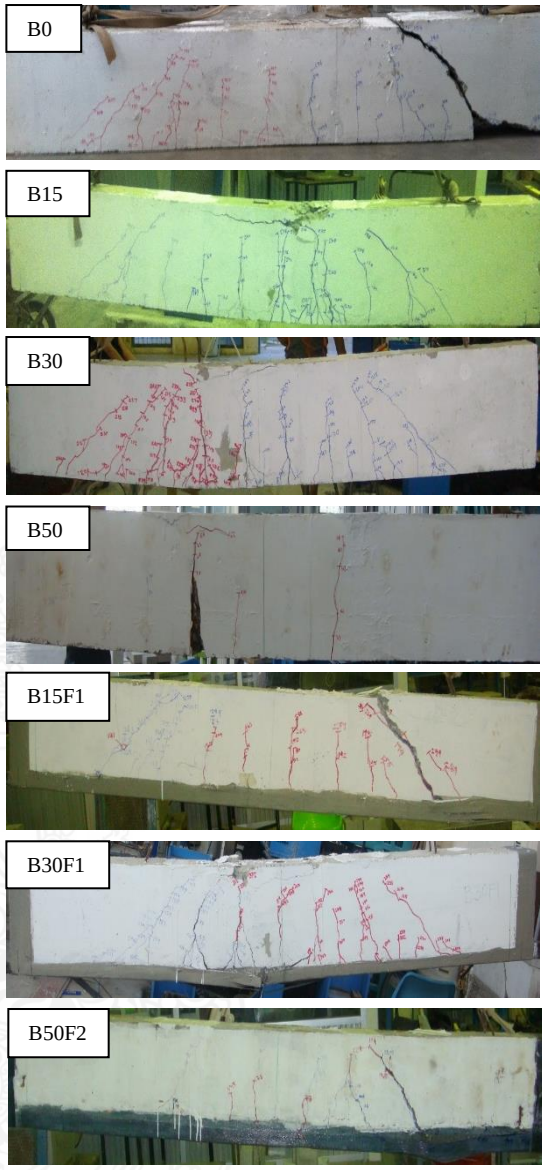

Fig. 8 Crack patterns and failure modes of test specimens

corroded tensile bars. Specimens B15F1, B30F1, and B50F2 have the crack patterns similar to those of the previous group. The failure mode B15F1 and B50F2 can be described as Type 4 which failed by a combination of flexural failure of the bottom tensile reinforcement and shear failure with fracture of CFRP sheets at the support. However, B30F1 can be

pronounced as Type 1 which failed by flexural failure of the bottom tensile reinforcement and fracture of CFRP sheets at the middle of the beam span. It should be noted that there is no failure in epoxy material obviously noticed from the test. This maybe results from the additional CFRP sheets wrapped around the beam cross section at the supports.

Considering the load response, ductility, and failure modes together, it can be concluded that corrosion results to large corrosion cracks and spalling, which reduce the bond between steel reinforcement and concrete, thus decreasing the bending stiffness of the beams. Nevertheless, this effect is not so obvious as the loss of ductility and capacity.

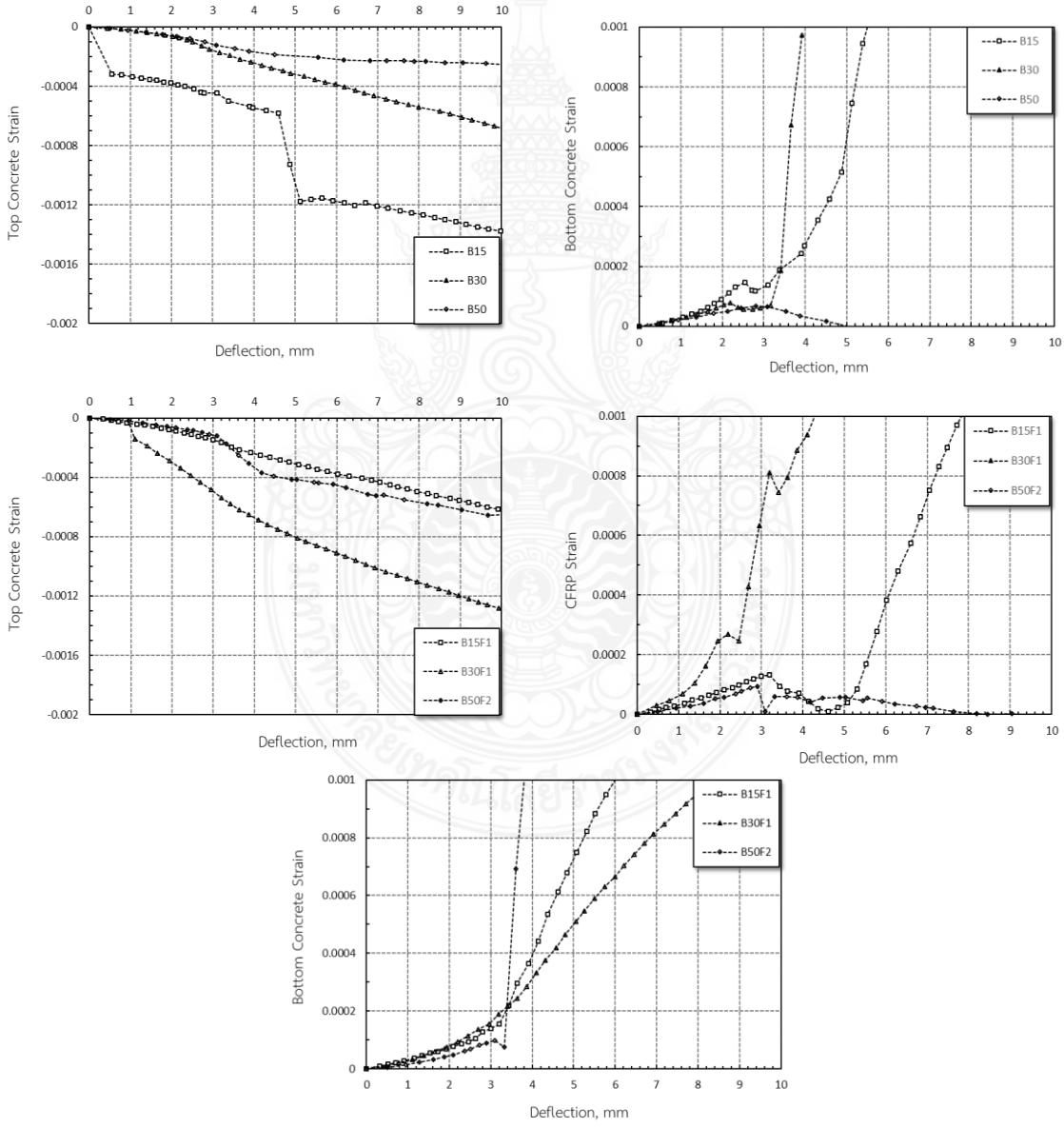

Fig. 9 Concrete and fiber strains for specimens

3.5 Concrete and CFRP Sheet Strains

In order to determine effectiveness of concrete and CFRP sheets, electrical strain gauges were attached to the top and bottom surface of concrete and also outer surface of the CFRP sheet as shown. **Fig. 9** illustrated variation of concrete and CFRP sheet strains against beam deflection. The results showed that concrete strain at the top surface of beams subjected to compressive loads clearly declined with increasing of the corrosion levels. The reversed behavior was detected for the bottom surface of beams, where concrete was in the tension zone. It was also noticed that higher degree of corrosion, lower activity of concrete was detected. This behavior caused from increasing of micro-crack inside the concrete with higher degrees of corrosion. When those specimens subjected to loads, the tension force quickly transferred to the tensile steels. This phenomenal leaded to sharply drop of the concrete strain with progress of the deflection. For the repaired specimens with CFRP sheets attached to the bottom surface of the beams, the gauges on CFRP sheets obviously confirmed the activity in tensile stress of the CFRP sheet. However, the study showed an inconclusive result to relate the levels of corrosion and activity of concrete strains causing from CFRP sheets. Therefore, the future study on this topic needs to be conducted.

4. Conclusion

The main conclusions drawn from the experiment are as follows:

1) The electrochemical process to accelerate corrosion in steel reinforcements of the RC beams successfully represents the corrosion behavior to the RC beams in the nature environments such as cracking of concrete, etc.

2) The corrosion levels predicted by Faraday's law well agree with results from the experiment.

3) Significant deteriorations in the yield capacity, ultimate capacity, and ductility are recorded due to the corrosion.

4) The test results indicate that significant gain in the flexural strength can be achieved by the bonding CFRP sheets to the tension surface of the corroded beams by up to 92%.

5) The use of CFRP sheets as an externally bonded to the bottom surface of the repaired RC beams proves to be efficient and provides sufficient in terms of strength and ductility for the low corrosion beams.

6) ACI 318 design provision underestimates the ultimate loads from the experiment by 44%-54% with the low corrosion beams, B15 and B30, and overestimates by 11% with the high corrosion beam, B50.

7) ACI 440.2R design provision slightly underestimates the ultimate loads by margin of 7% for beams B15F1 and B30F1, and significantly overestimates the ultimate capacity of B50F2 by 102%.

Finally, the future study needs to be carried on evaluation of the ultimate flexural and shear capacity of the corroded steel reinforcement beams repaired with the externally bonded CFRP sheets,

especially with the high degree of corrosion-damaged RC beams.

5. Acknowledgement

Authors would like to thank all former students and technician staffs of department of civil engineering, Burapha University, who made contribution in anyways to this study. Also, sincerely thank would be extended to the research and innovation administration division at Burapha University for all supports. This study is financially supported by a grant from engineering school, Burapha University, (Contract no. 62/2552).

6. References

[1] P. Mangat and M. Elgarf, "Flexural Strength of concrete beams with corroding reinforcement," *ACI Struct. J.*, vol. 96, pp. 149-158, 1999.

[2] Y. Ballim and J. Reid, "Reinforcement corrosion and the deflection of RC beams-an experimental critique of current test methods," *Cem. Concr. Compos. J.*, vol. 25, pp. 625-632, 2003.

[3] M. Goitseone, A. Mark and M. Pilate, "Variation of steel loss and its effect on the ultimate flexural capacity of RC beams corroded and repaired under load," *Constr. Build. Mater.*, vol. 24, pp. 1051-1059, 2010.

[4] X. Gu, W. Zhang and D. Shang, "Flexural Behavior of Corroded Reinforced Concrete Beams," in *Proceedings of the 12th Biennial International Conference on Engineering, Construction, and Operations in Challenging Environments*, Honolulu, HI, USA, 2010.

[5] W. Zhu, R. François, D. Coronelli and D. Cleland, "Effect of corrosion of reinforcement on the mechanical behavior of highly corroded RC beams," *Eng. Struct. J.*, vol. 56, pp. 544-554, 2013.

[6] A. Torres-Acosta, M. Fabela-Gallegos, A. Munoz-Noval, D. Vazquez-Vega, T. Hernandez-Jimenez and M. Martinez-Madrid, "Influence of corrosion on the structural performance of reinforced concrete beams," *Corrosion*, vol. 60, pp. 862-872, 2004.

[7] A. Al-Saidyn and K. Al-Jabri, "Effect of damaged concrete cover on the behavior of corroded concrete beams repaired with CFRP sheets," *Compos. Struct.*, vol. 93, pp. 1775-1786, 2011.

[8] R. Haddad, "Hybrid repair configurations with CFRP composites for recovering structural performance of steel-corroded beams," *Construction and Building Materials*, vol. 124, pp. 508-518, 2016.

[9] J. Rodriguez, L. Ortega and J. Casal, "Load Carrying Capacity of Concrete Structures with Corroded Reinforcement," *Constr. Build. Mater.*, vol. 11, pp. 239-248, 1997.

[10] *ASTM G1.*, "Standard Practice for Preparing, Cleaning, and Evaluating Corrosion Test Specimens," *American Society for Testing and Materials: West Conshohocken*, PA, USA, 2003.

[11] *ACI Committee 318-14.*, "Building Code Requirements for Structural

Concrete," American Concrete Institute: Farmington Hills, MI, USA, 2014.

[12] *ACI Committee 440.2R-17.*, "Guide for the Design and Construction of Externally Bonded FRP Systems for Strengthening Concrete Structures," American Concrete Institute: Farmington Hills, MI, USA, 2017.

[13] J. MacGregor and J. Wight, "*Reinforced Concrete Mechanics and Design*," 4th ed. Boston: Pearson, 2005.